Available online at www.sciencedirect.com
SCIENCE DIRECT®
Journal of Luminescence 107 (2004) 194–202
JOURNAL OF LUMINESCENCE
www.elsevier.com/locate/jlumin

Electron–phonon coupling in two-photon spectral gratings: role of molecular symmetry

M. Drobizhev[a,b,*], Yu. Dzenis[a], A. Karotki[a], A. Rebane[a]

[a] Department of Physics, Montana State University, Bozeman, MT 59717-3840, USA
[b] Lebedev Physics Institute, Leninsky pr., 53, Moscow 119991, Russia

Abstract

We study spectral gratings obtained as a result of two-photon excitation of the lowest electronic transition of several tetrapyrrole molecules with phase-locked pairs of femtosecond pulses. A particular dependence of these gratings on temperature indicates that mirror symmetry is present between two-photon absorption (TPA) and one-photon fluorescence spectra for non-centrosymmetrical chlorin, but fails for centrosymmetrical naphthalocyanine. The latter case is best described if the homogeneous TPA spectrum contains phonon sideband, but not the zero-phonon line. These results are discussed in terms of alternative selection rules for one- and two-photon transitions in centrosymmetrical molecules.

Keywords: Two-photon absorption; Two-photon coherence; Zero-phonon lines; Spectral hole burning; Herzberg–Teller interaction; Parity selection rules

1. Introduction

In our previous papers [1–3], we have demonstrated the possibility of creating spectral gratings as a result of two-photon absorption (TPA) in inhomogeneously broadened media at low temperatures. Intuitively, this effect implies the presence of narrow zero-phonon lines (ZPL) in TPA transition. TPA pure electronic ZPLs were shown for several molecules, including centrosymmetric [4–10] and non-centrosymmetric ones [11,12].

For non-centrosymmetric molecules, the same transition is simultaneously allowed for one-photon absorption and TPA and, therefore, the same pure electronic ZPL can be observed in both types of transition. For example, one can observe the pure electronic ZPL in one-photon fluorescence spectrum upon two-photon excitation of the very same transition. For centrosymmetric molecule (in centrosymmetric site), selection rules for two- and one-photon transitions are mutually exclusive and, therefore, the role of vibrations and matrix phonons becomes decisive.

Similarly to one-photon case (exemplified by photon echo and time-domain holography), in TPA-induced gratings, two fs pulses, delayed by time $\Delta\tau$, are applied to a material, thus resulting in interference and interference fringes in frequency dimension [1–3]. However, in contrast to usual one-photon case, photons are absorbed by pairs from each pulse. Two-photon excitation has

*Corresponding author. Department of Physics, Montana State University, Bozeman, MT 59717-3840, USA.
E-mail address: drobizhev@physics.montana.edu (M. Drobizhev).

0022-2313/$ - see front matter © 2004 Elsevier B.V. All rights reserved.
doi:10.1016/j.jlumin.2003.12.032

potential advantage in several applications, including ultrahigh-density optical memory (3D memory of ultrafast temporal processes) and ultrafast optical computing.

If the homogeneous spectrum of impurity system consists only of narrow ZPL, the spectral response of the medium is exactly the replica of power spectrum of Fourier transform of the square of electric field temporal profile [2,3]. For a series of short pulses, the total spectral width is determined by the inverse pulse duration. Organic systems, such as polymer films doped with organic molecules, present an optimum recording media for 100 fs duration laser pulses because the inhomogeneous broadening in these systems is of the order of the inverse pulse duration. However, almost all organic systems show considerable phonon wings (PWs) in their homogeneous spectra with ZPL–PW separation less than inhomogeneous width. Therefore, an important problem, which needs to be considered in connection with TPA gratings and their practical applications, is the effect of low-frequency phonons on the shape of TPA-induced spectral gratings. TPA electron–phonon transitions become dominant for centrosymmetric molecules, where pure electronic transition (ZPL) is forbidden by symmetry.

In this paper we consider TPA gratings created in different molecular systems, with and without center of inversion. The spectral fringes are excited with photons of energy equal to one-half the first S_0S_1 transition energy and monitored in fluorescence of the same S_0S_1 transition. As compared to our previous paper [3], here we elaborate a model, which considers homogeneous TPA spectrum independently of homogeneous fluorescence spectrum, i.e. we do not restrict ourselves to mirror-symmetrical case. We quantitatively simulate the observed temperature dependence of spectral fringes and show that for centro-symmetric naphthalocyanine molecule the best result can be obtained if the Debye–Waller factor of homogeneous TPA spectrum tends to zero. On the other hand, in non-centrosymmetric chlorin (Chl) molecule the fringes are described well by a model where the TPA spectrum is mirror symmetrical to one-photon fluorescence spectrum.

2. Experimental setup and materials

The details of our experimental setup have been previously described in Ref. [3]. Briefly, the laser system comprised a 1 kHz repetition rate Ti:sapphire regenerative amplifier system (Clark MRX CPA-1000) seeded by a mode-locked Ti:sapphire femtosecond laser (Coherent Mira 900). The amplified pulses had duration of 150 fs and energy of 0.8 mJ at 780 nm. TOPAS (Quantronix) optical parametric amplifier (OPA) was used to convert 780 nm pulses into near-IR pulses tunable in the range 1100–1600 nm. These pulses were nearly Fourier-transform limited, had duration 100 fs and energy 0.1–0.2 mJ. Glass color filters were used to cut off any residual visible light from the OPA. A Michelson interferometer divided the OPA beam into two spatially overlapped but time-delayed beams. Time delay between the two pulses was set $\Delta\tau = 700$ fs. The pulses were focused with an $f = 500$ mm lens onto a sample positioned inside a variable-temperature (2–300 K) helium bath cryostat.

Fluorescence was collected with a spherical mirror and focused on the entrance slit of a Jobin-Yvon TRIAX 550 spectrometer equipped with an N_2-cooled CCD array detector.

We used 0.2-mm thick polyvinylbutyral (PVB) films activated with tetrapyrrole molecules at a concentration of about 10^{-4} mol/l. 7,8-dihydroporphyrin (Chl) was obtained from Swiss Federal Institute of Technology (Zürich), silicon-2, 3-naphthalocyanine dioctyloxide (SiNc) was purchased from Aldrich, phthaloanthracenocyanine (Pc_3An, Ciba 1009) was obtained from Ciba.

3. Experimental results

Fig. 1 shows fluorescence spectra of the three molecules in PVB at $T = 4$ K, recorded in the region corresponding to the inhomogeneously broadened 0–0 transition upon excitation with near-IR pulses of wavelength twice the absorption maximum. One can see that if the sample is illuminated with pairs of phase-locked pulses, the part of the spectrum around the laser carrier frequency shows distinct spectral fringes (solid

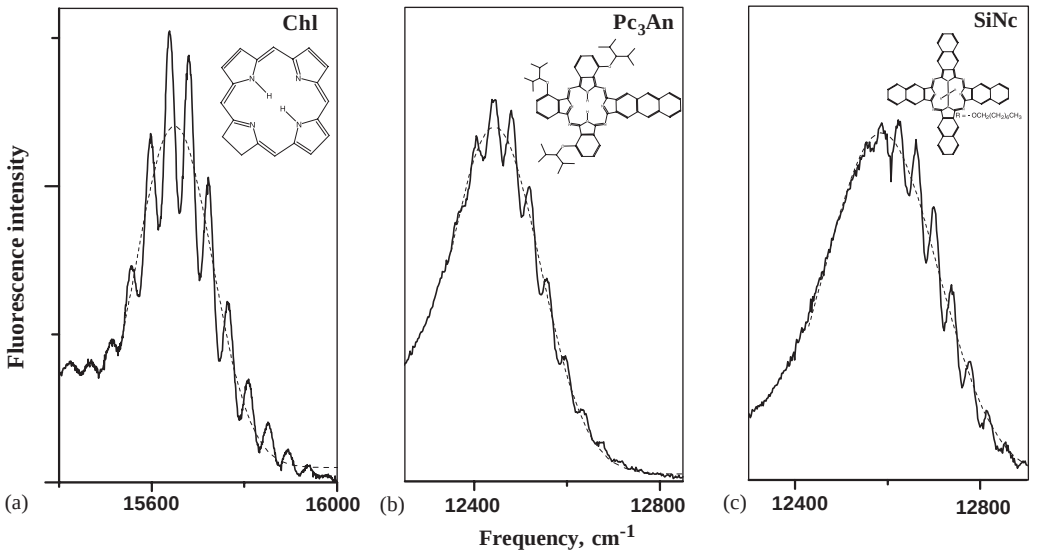

Fig. 1. S_1-S_0 fluorescence spectra of Chl- (a), anthracenophthalocyanine- (b) and Si-naphthalocyanine- (c) doped PVB films obtained at 4 K upon excitation with pairs of near-IR femtosecond pulses. Dashed line in each plot is the best Gaussian fit to the spectrum.

curve). The period of fluorescence intensity modulation is $40\,\mathrm{cm}^{-1}$, which corresponds exactly to the inverse delay between pulses ($\Delta\tau = 700$ fs). A smooth dashed curve is a Gaussian fit to fluorescence spectrum, corresponding to the spectrum excited non-coherently. Fig. 2 shows a typical laser spectrum coming out of Michelson interferometer and used for TPA excitation. This spectrum is recorder with a Lambda 900 Perkin-Elmer spectrophotometer and can be described by Fourier transform of two Gaussian pulses separated by $\Delta\tau$:

$$L(\nu') = G\exp(-(\nu'-\nu_{\mathrm{L}})^2/(\delta\nu')^2)(1+\beta\cos(2\pi\nu'\Delta\tau)), \quad (1)$$

where G is a constant, ν_{L} is the carrier frequency, $\delta\nu'$ is the spectral width of laser pulse, β is the modulation depth of excitation, which depends on the relative amplitude of the two pulses. If the amplitudes are the same, $\beta = 1$, and $\beta < 1$ otherwise. From the plot, presented in inset, we find the depth of excitation modulation $\beta = 0.75$.

Returning to Fig. 1, we can note a very interesting fact that larger one-photon Debye–Waller factor, α_1, does not result in higher contrast of fringes, all other condition being the same.

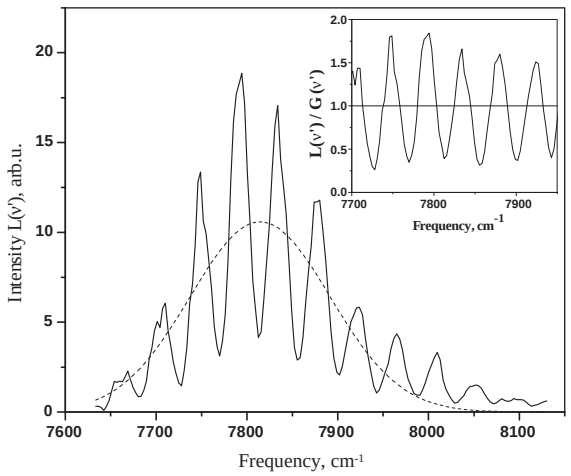

Fig. 2. Excitation laser spectrum, coming out Michelson interferometer and recorded with a slow detector of spectrophotometer. Dashed line is the Gaussian envelope of this spectrum, corresponding to the broad envelope in Eq. (1): $G(\nu'-\nu_L) = G\exp(-(\nu'-\nu_L)^2/(\delta\nu')^2)$. The ratio of modulated spectrum to this Gaussian envelope, $1+\beta\cos(2\pi\nu'\Delta\tau)$, is shown in inset. From this plot we find the depth of excitation modulation $\beta = 0.75$.

Indeed, the largest modulation depth, $M = 0.32$, is observed for Chl, where $\alpha_1 = 0.55$ [13]. On the other hand, SiNc, with much higher $\alpha_1 \approx 1.0$ [14],

shows even smaller modulation depth, $M = 0.24$. The lowest $M = 0.15$ is observed for Pc_3An, where the Debye–Waller factor ($\alpha_1 = 0.63$ [15]) is larger than that of Chl. This first observation can suggest the important role of molecular symmetry in TPA-induced gratings. More specifically, it seems that molecules with broken inversion symmetry demonstrate deeper TPA fringes (sharper homogeneous TPA spectrum) than molecules possessing center of inversion, cf. Chl and SiNc. The case of Pc_3An can be considered as an intermediate one, since the main electronic conjugation path in tetrapyrrolic ring is not broken (cf. chlorin), but *mono*-anthraceno substitution can introduce certain asymmetry. By comparing the modulation contrast in Fig. 1, we can just qualitatively estimate at this moment that the sharpness of TPA spectrum of Pc_3An is closer to that of SiNc.

To get more insight into the role of molecular symmetry in homogeneous TPA spectrum, we measured the temperature dependence of TPA fringes in two extreme cases, i.e. for symmetrical SiNc and non-symmetrical Chl. The results are presented in Fig. 3. In both cases, an increase of temperature results in diminishing contrast of the fringes. The striking difference between the two systems is that in Chl the fringes shift to the red with increasing temperature, whereas in SiNc this shift is much less pronounced. Indeed, for Chl the observed shift of the grating constitutes a half of its period upon increasing temperature from 4 to 60 K. We checked that this shift was completely reversible when temperature was lowered down to 4 K again, thus ensuring that it is inherent property of the sample.

In order to quantitatively simulate the temperature dependence of TPA-induced gratings, presented in Fig. 3, we have elaborated a simple model described in the next section.

4. The model

The fluorescence spectrum of an inhomogeneously broadened ensemble of molecules, excited by light with two-photon "action" spectrum $I(\nu'')$ (proportional to the square of the Fourier transform of the electric field squared [2,3]) is

$$F(\nu, T) = \int_{-\infty}^{\infty} N(\nu_0) g_1(\nu - \nu_0, T)\, d\nu_0 \times \int_{-\infty}^{\infty} g_2(\nu'' - \nu_0, T) I(\nu'')\, d\nu'', \quad (2)$$

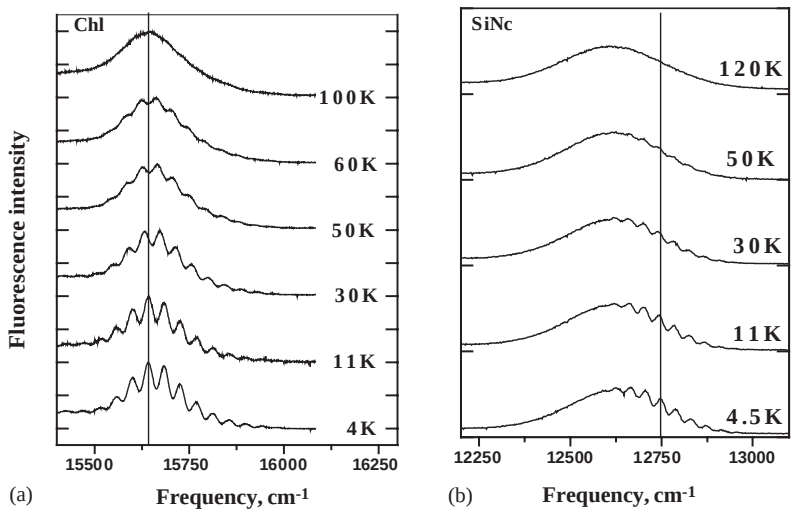

Fig. 3. S_1-S_0 fluorescence spectra of Chl- (a) and Si-naphthalocyanine- (b) doped PVB film obtained at different temperatures upon excitation with pairs of femtosecond pulses. Vertical line in each plot correspond to one selected peak in the grating at lowest temperature. For Chl, a large red shift of the grating is observed at increasing temperature, whereas for SiNc this shift is much smaller.

where $g_2(\nu-\nu_0,T)$ is the homogeneous TPA spectrum, $g_1(\nu-\nu_0,T)$ is the homogeneous one-photon fluorescence spectrum with ZPL frequency ν_0, and $N(\nu_0)$ is the inhomogeneous distribution function. A slowly varying spectral function, including the excitation spectrum envelope and the inhomogeneous distribution function, which are both much broader than the grating period, ZPL, and PW, can be considered as a constant and brought out of the integral in Eq. (2). In this approximation, we can write for excitation spectrum [2,3]

$$I(\nu'') = 1 + \beta\cos(2\pi\nu''\Delta\tau). \tag{3}$$

As usual, we describe the homogeneous (two-photon) absorption and (one-photon) fluorescence spectra as a sum of ZPL and PW

$$g_{1,2}(\nu-\nu_0,T) = \alpha_{1,2}(T)\delta(\nu-\nu_0) + [1-\alpha_{1,2}(T)]p_{1,2}(\nu-\nu_0), \tag{4}$$

where $\alpha_{1,2}(T)$ is the Debye–Waller factor, indexes 1 and 2 designate fluorescence and absorption, respectively, ZPL is represented by delta function, and PW is described by the following model function:

$$p_{1,2}(\nu-\nu_0) = \begin{cases} \dfrac{4}{\nu_{1,2}^3}(\nu_0-\nu)^2\exp[\mp\frac{2}{\nu_{1,2}}(\nu_0-\nu)], & \pm(\nu_0-\nu)>0, \\ 0, & \pm(\nu_0-\nu)\leqslant 0, \end{cases} \tag{5}$$

where the upper sign is for fluorescence, the lower sign is for absorption, $\nu_{1,2}$ is the maximum of spectral distribution of PW. The validity of approximation (5) is supported by a satisfactory fit of pseudophonon wing to Eq. (5) in standard hole-burning experiment with Chl and SiNc in PVB (see Fig. 4). Function (5) includes only one adjustable parameter, $\nu_{1,2}$, which does not depend on temperature in our model. The best fit (at $T=4-30\,\mathrm{K}$) gives $\nu_1 = 18\,\mathrm{cm}^{-1}$ for Chl and $\nu_1 = 14\,\mathrm{cm}^{-1}$ for SiNc, which agrees well with previous hole-burning [15,16] and Raman scattering [17] results for PVB. We assume the effect of temperature broadening of PWs is negligible, which is justified experimentally [18] in the same temperature range (4–100 K) as in our experiments. All the temperature dependence is then contained in Debye–Waller factor, which we treat in one-oscillator approximation as

$$\alpha_{1,2}(T) = \exp\left(-\xi_{1,2}\mathrm{cth}\left(\frac{h\nu_{1,2}}{2kT}\right)\right), \tag{6}$$

where ξ is the electron–phonon coupling strength.

Substituting Eqs. (5) and (6) into Eq. (4) and then Eqs. (3) and (4) into Eq. (2) and performing integration, we get the following expression for

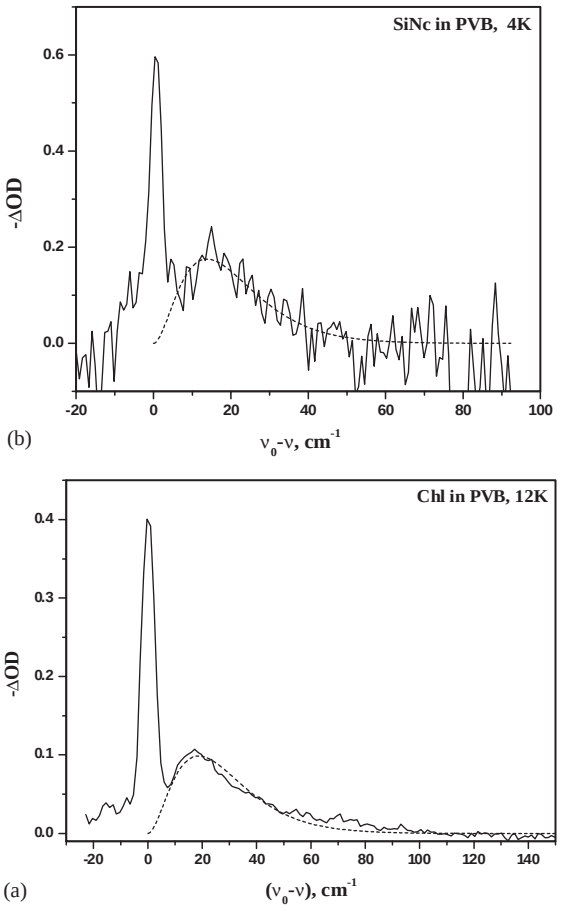

Fig. 4. Spectral hole profiles for Chl (a) and SiNc (b) in PVB. Holes are burnt with He–Ne and cw Ti:sapphire lasers, respectively. A ratio of integrated ZPL and PW does not reflect the Debye–Waller factor, since zero-phonon hole is already saturated. However, pseudophonon sideband (to the right of ZPL) reasonably reflects the PW profile. A fit of its profile to function (5) is shown by dashed line on each plot.

fluorescence spectrum:

$$F(v,T) = K(v)[1 + M(T)\cos(2\pi\Delta\tau v + \Delta\varphi(T))], \quad (7)$$

where the amplitude $M(T)$ and the phase shift $\Delta\varphi(T)$ of the grating are given by

$$M(T) = \beta\{[A + B\cos\delta_2 + C\cos\delta_1 + D\cos(\delta_1+\delta_2)]^2 + [B\sin\delta_2 + C\sin\delta_1 + D\sin(\delta_1+\delta_2)]^2\}^{1/2}, \quad (8)$$

$$\Delta\varphi(T) = \mathrm{arctg}\frac{B\sin\delta_2 + C\sin\delta_1 + D\sin(\delta_1+\delta_2)}{A + B\cos\delta_2 + C\cos\delta_1 + D\cos(\delta_1+\delta_2)}. \quad (9)$$

Here functions $A(T)$, $B(T)$, $C(T)$, and $D(T)$ are expressed through the model parameters as follows:

$$A(T) = \alpha_1(T)\alpha_2(T), \quad (10)$$

$$B(T) = [1-\alpha_1(T)]\alpha_2(T) \times \{1 + (\pi\Delta\tau v_2)^2\}^{-3/2}, \quad (11)$$

$$C(T) = \alpha_1(T)[1-\alpha_2(T)] \times \{1 + (\pi\Delta\tau v_1)^2\}^{-3/2}, \quad (12)$$

$$D(T) = [1-\alpha_1(T)][1-\alpha_2(T)] \times \{[1 + (\pi\Delta\tau v_2)^2][1 + (\pi\Delta\tau v_1)^2]\}^{-3/2} \quad (13)$$

and

$$\delta_{1,2} = 3\,\mathrm{arctg}(\pi\Delta\tau v_{1,2}). \quad (14)$$

We note here that in the limiting case $\alpha_1(0) = \alpha_2(0) = 1$ Eq. (9) does give a quantitatively correct phase shift, $\Delta\varphi(0) = 0$. However, for example, for $\alpha_1 = \alpha_2 = 0$, the correct behavior is reproduced only at small $\pi\Delta\tau v_{1,2}$: $\Delta\varphi = 3\pi\Delta\tau(v_1 + v_2)$. This last value corresponds to a frequency shift (Stokes shift) of $\Delta v = \frac{3}{2}(v_1 + v_2)$, equal to a difference between centers of gravity of PWs (5) in absorption and fluorescence. In general case, the values of $\Delta\varphi$ allowed by Eq. (9) are restricted by definition of function $\mathrm{arctg}(x)$, and, therefore, Eq. (9) is unable to describe a wide range of other real sets of parameters. In our approach we use Eq. (8) for the simulation of the temperature dependence of the amplitude (contrast) of the fringes, but we resort to a simpler model for the simulation of the temperature dependence of the phase. We consider the Stokes shift as a difference between the first moments (centers of gravity) of absorption and fluorescence homogeneous spectra, namely,

$$\Delta v(T) = (1-\alpha_2(T))v_2 + (1-\alpha_1(T))v_1, \quad (15)$$

and, therefore,

$$\Delta\varphi(T) = 2\pi\Delta\tau[(1-\alpha_2(T))v_2 + (1-\alpha_1(T))v_1]. \quad (16)$$

5. Results of simulations and discussion

5.1. Chl in PVB

First of all, we simulated the temperature dependence of the fringes in Chl:PVB system by using symmetrical model with $\xi_1 = \xi_2 = \xi$ and

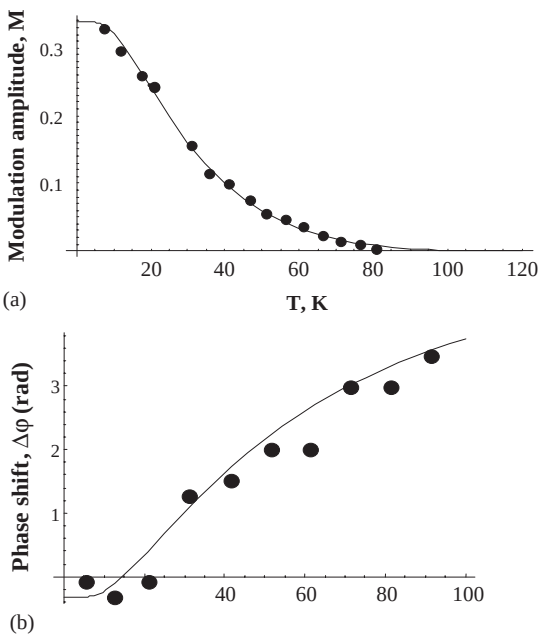

Fig. 5. Temperature dependence of the amplitude M (a) and phase shift $\Delta\varphi$ (b) of spectral grating observed in Chl:PVB and corresponding fits of these data to Eqs. (8) and (16) in mirror-symmetrical model.

$\nu_1 = \nu_2 = \nu_m$. By varying two adjustable parameters, ξ and ν_m, we obtain the best fit, shown in Fig. 5a, at $\xi = 0.36$, (i.e. $\alpha_1(0) = \alpha_2(0) = 0.70$) and $\nu_m = 25\,cm^{-1}$. Substitution of these parameters into Eq. (16) without any further fitting gives a phase shift, shown in Fig. 5b by solid line. One can conclude that the model fits well in this case and the obtained parameters are reasonable. The value of ν_m is slightly larger than the maximum phonon frequency ($18\,cm^{-1}$), but it is very close to a center of gravity of PW distribution, which can be a real effective frequency entering Eq. (6). The limiting Debye–Waller factor $\alpha_1(0)$ agrees well with the value measured at 7 K ($\alpha_1 = 0.55$) in Ref. [13].

We then performed the fit procedure of the same data but using the asymmetrical model, where all four parameters ξ_1, ξ_2, ν_1, and ν_2 were varied independently. The best fit of $M(T)$ (Fig. 6a), and $\Delta\varphi(T)$ (Fig. 6b), do, in fact, describe the experiment quite well, but the limiting Debye–Waller factor $\alpha_1(0) = 0.86$ comes out much larger than the literature data, cited before. The main conclusion, which can be drawn from the simulation obtained for Chl:PVB is that the symmetrical model works quite well for this system.

5.2. SiNc in PVB

The simulation of experimental data for SiNc:PVB with mirror-symmetrical model is shown in Figs. 7a and b. Again, the fit procedure was first accomplished for the amplitude and then the best parameters were introduced in Eq. (16) to describe the phase shift. The main inconsistency between the simulation and experiment is observed in the phase behavior, because the model tends to overestimate the rate of the shift with temperature. The obtained best-fit parameters also differ considerably from literature data: the limiting value of Debye–Waller factor ($\alpha_1(0) = 0.56$) is way too small as compared to that reported previously ($\alpha_1 = 1.0$ at 1.5 K) [14] and the characteristic

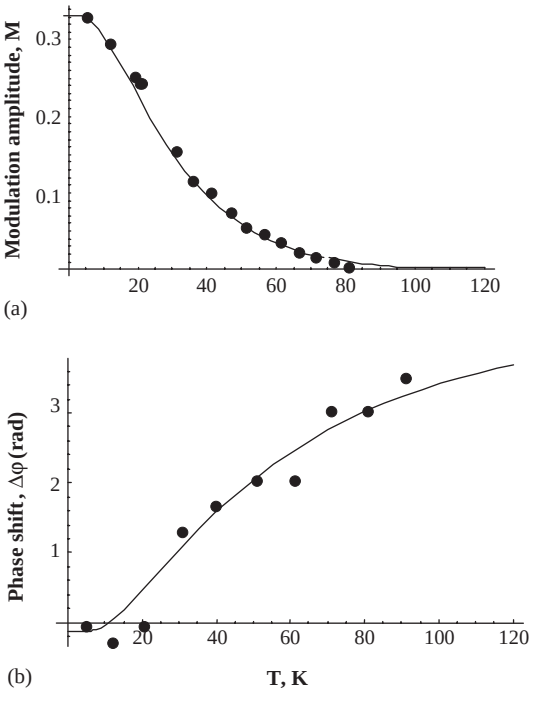

Fig. 6. Temperature dependence of the amplitude M (a) and phase shift $\Delta\varphi$ (b) of spectral grating observed in Chl:PVB and corresponding fits of these data to Eqs. (8) and (16) in non-mirror-symmetrical model.

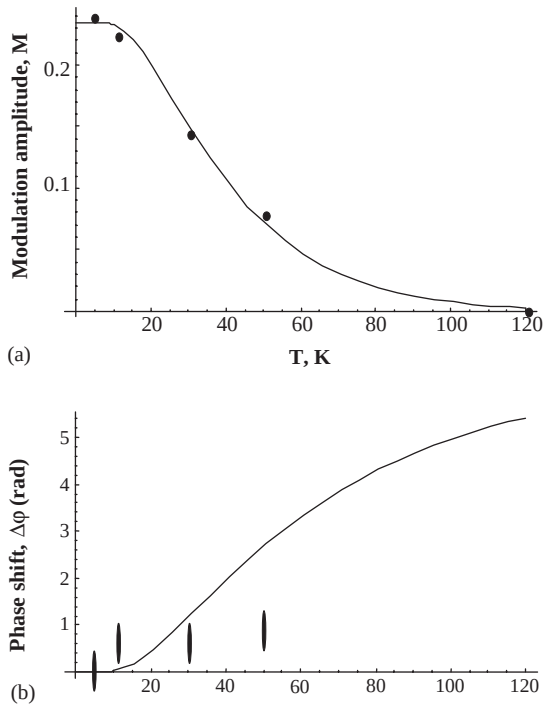

Fig. 7. Temperature dependence of the amplitude M (a) and phase shift $\Delta\varphi$ (b) of spectral grating observed in SiNc:PVB and corresponding fits of these data to Eq. (8) and (16) in mirror-symmetrical model.

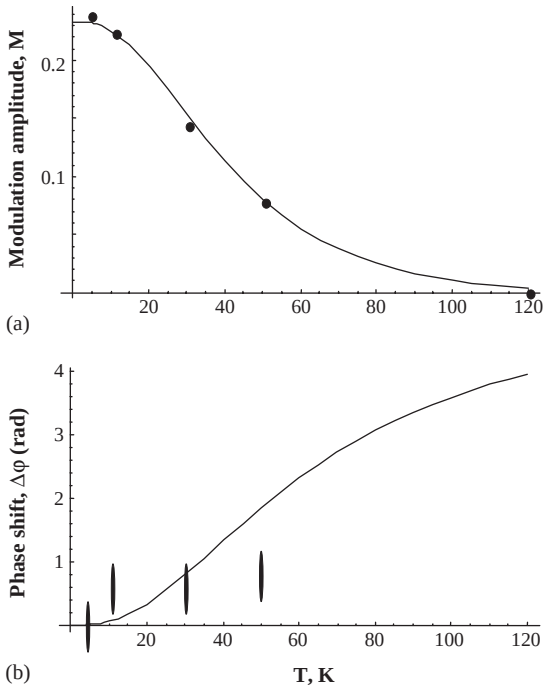

Fig. 8. Temperature dependence of the amplitude M (a) and phase shift $\Delta\varphi$ (b) of spectral grating observed in SiNc:PVB and corresponding fits of these data to Eq. (8) and (16) in non-mirror-symmetrical model.

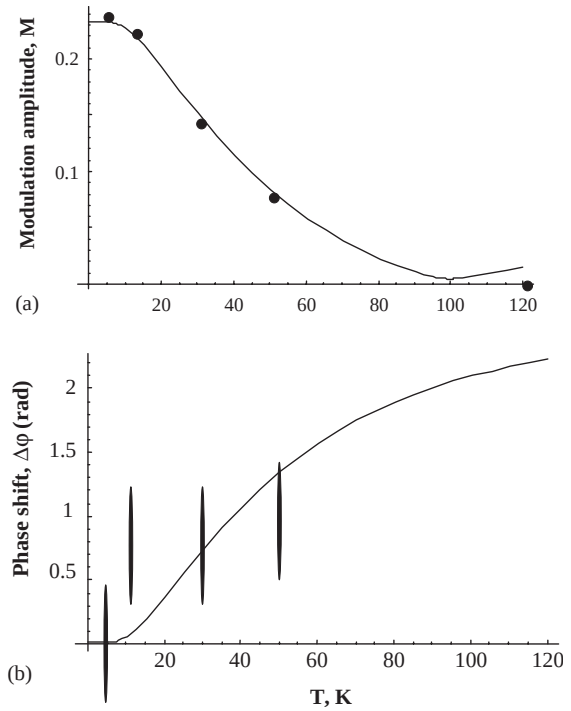

Fig. 9. Temperature dependence of the amplitude M (a) and phase shift $\Delta\varphi$ (b) of spectral grating observed in SiNc:PVB and corresponding fits of these data to Eq. (8) and (16) in non-mirror-symmetrical model, where the Debye–Waller factor for TPA (α_2) was set to zero.

phonon frequency $\nu_m = 39\,cm^{-1}$ seems to be overestimated.

Our next attempt was to simulate the data with asymmetrical model with four independent parameters (Figs. 8a and b). One-photon parameters were fixed to the values, known from hole-burning spectroscopy: $\alpha_1(0) = 0.9$ and $\nu_1 = 17\,cm^{-1}$, and ξ_2 and ν_2 were varied. The best fitting values obtained for these parameters are $\xi_2 = 1.0(\alpha_2(0) = 0.37)$ and $\nu_2 = 56\,cm^{-1}$. It is obvious that this fit fails again in describing the phase shift of Fig. 8b.

We could obtain a reasonably good fit (Figs. 9a and b) only if we artificially set $\alpha_2(T) = 0(\xi_2 = 10\,000)$ and let other three parameters vary independently. This implies no ZPL in TPA spectrum even at the lowest temperature. For the emission spectrum we obtain reasonable $\xi_1 = 0.46$ and $\nu_1 = 27\,cm^{-1}$, while the Debye–Waller factor again occurs smaller than measured in Ref. [14] (0.63 vs 1.0). Note that the homogeneous TPA spectrum turns out to be strongly asymmetric with respect to homogeneous one-photon emission spectrum. Not only does this absorption contain no ZPL ($\alpha_2(0) = 0$), but its PW is shifted by only $\nu_2 = 10\,cm^{-1}$ from the zero-phonon origin.

Several important conclusions can be drawn from these observations. First of all, mirror-symmetric spectral model works well for Chl. This is not very surprising result because this molecule does not possesses the center of inversion, and, therefore, selection rules for one- and two-photon transitions should be the same. On the other hand, TPA gratings in SiNc:PVB system are best described by strongly asymmetrical model in which ZPL of TPA is completely missing. This fact can be explained if we consider selection rules for pure electronic transition in this centro-symmetrical molecule. Since we are dealing with *gerade* $\leftrightarrow$ *ungerade*, $S_0 \leftrightarrow S_1$ one-photon transition, it must be strongly forbidden for pure electronic

TPA [4–10]. However, TPA with creation of phonons (electron–phonon transition, building up PW in homogeneous TPA spectrum) can be allowed through Herzberg–Teller mechanism. In this case, TPA grating can be created on pure phonon coherences. It is, of course, evident that for the observation of the fringes, the phonon coherence time, T_2, must be comparable or longer than the time delay between pulses, $\Delta\tau$· It is known from femtosecond photon echo experiments [17,18] that the phonon coherence time in polymer matrices at low temperatures ranges from several hundred of fs to 1 ps. In our experiments we use $\Delta\tau = 700$ fs, which is a sufficiently small value to produce spectral interference on phonon coherences, at least in SiNc:PVB system. From the other side, one cannot reduce $\Delta\tau$ to an arbitrarily small value, since it is limited from below by inverse inhomogeneous width, which is of the order of 100 fs. Therefore, there exists a limited range of delays ($\Delta\tau \sim 100-1000$ fs), where TPA gratings can be observed in the case of absence of ZPLs in a system.

6. Conclusion

Temperature dependence of spectral interference fringes, obtained by two-photon excitation of the lowest electronic molecular transition with phase-locked pairs of femtosecond pulses is studied. Mathematical simulation of this dependence demonstrates that Franck–Condon model with mirror symmetrical TPA and one-photon fluorescence spectra works well for non-centrosymmetrical chlorin, but fails for centrosymmetrical naphthalocyanine. In the later case, the dependence is best described by a model where homogeneous TPA spectrum does not contain ZPL. These results can be explained by similar selection rules for one- and two-photon transitions in non-centrosymmetrical molecules, but alternative ones for centrosymmetrical molecules. Therefore, in the later case only electron–phonon transitions are allowed and the TPA gratings can be observed only if the time delay between the pulses is still shorter than phonon dephasing time.

Acknowledgements

This work was supported by AFOSR Grant F49620-01-0406.

References

[1] M. Drobizhev, A. Karotki, A. Rebane, Chem. Phys. Lett. 334 (2001) 76.
[2] A. Karotki, M. Kruk, M. Drobizhev, A. Rebane, J. Mod. Opt. 49 (2002) 379.
[3] A. Rebane, M. Drobizhev, A. Karotki, J. Lumin. 98 (2002) 341.
[4] R.M. Hochstrasser, H.N. Sung, J. Chem. Phys. 66 (1977) 3265.
[5] R.M. Hochstrasser, H.N. Sung, J. Chem. Phys. 66 (1977) 3276.
[6] N. Mikami, M. Ito, Chem. Phys. 23 (1977) 141.
[7] M.F. Granville, G.R. Holtom, B.E. Kohler, R.L. Christensen, K.L. D'Amico, J. Chem. Phys. 70 (1979) 593.
[8] M. Gutmann, P.-F. Schonzart, G. Hohlneicher, Chem. Phys. Lett. 140 (1990) 107.
[9] T. Plakhotnik, D. Walser, A. Renn, U.P. Wild, Chem. Phys. Lett. 262 (1996) 379.
[10] D. Walser, G. Zumofen, T. Plakhotnik, J. Chem. Phys. 113 (2000) 8047.
[11] M.C. Edelson, J.M. Hayes, G.J. Small, Chem. Phys. Lett. 60 (1979) 307.
[12] M. Takeda, K. Matsuda, C. Suzuki, S. Saikan, J. Lumin. 86 (2000) 285.
[13] W.-I. Huang, A. Rebane, U.P. Wild, L.W. Johnson, J. Lumin. 71 (1997) 237.
[14] A.V. Turukhin, A.A. Gorokhovsky, C. Moser, I.V. Solomatin, D. Psaltis, J. Lumin. 86 (2000) 399.
[15] I. Renge, H. Wolleb, H. Spahni, U.P. Wild, J. Phys. Chem. A 101 (1997) 6202.
[16] I. Renge, J. Chem. Phys. 106 (1997) 5836.
[17] S. Saikan, J. Lumin. 53 (1992) 147.
[18] A. Rebane, J. Gallus, O. Ollikainen, Laser Phys. 12 (2002) 1126.